Published in final edited form as:

*J Cell Physiol*. 2018 March ; 233(3): 2398–2408. doi:10.1002/jcp.26111.

# GSK-3β Inhibition Suppresses Instability-induced Osteolysis by a Dual Action on Osteoblast and Osteoclast Differentiation

**Mehdi Amirhosseini**[1], **Rune V. Madsen**[2], **K. Jane Escott**[3], **Mathias P. Bostrom**[2], **F. Patrick Ross**[2], and **Anna Fahlgren**[1,*]

[1]Department of Clinical and Experimental Medicine, Division of Cell Biology, Linköping University, 58185 Linköping, Sweden

[2]Adult Reconstruction and Joint Replacement Service, Hospital for Special Surgery, New York, New York

[3]Scientific Partnering & Alliances, Innovative Medicines and Early Development Biotech Unit, AstraZeneca, Melbourn Science Park, Cambridge Road, Melbourn, Herts SG8 6EE, UK

## Abstract

Currently, there are no medications available to treat aseptic loosening of orthopedic implants. Using osteoprotegerin fusion protein (OPG-Fc), we previously blocked instability-induced osteoclast differentiation and peri-prosthetic osteolysis. Wnt/β-catenin signaling, which regulates OPG secretion from osteoblasts, also modulates the bone tissue response to mechanical loading. We hypothesized that activating Wnt/β–catenin signaling by inhibiting glycogen synthase kinase-3β (GSK-3β) would reduce instability-induced bone loss through regulation of both osteoblast and osteoclast differentiation. We examined effects of GSK-3β inhibition on regulation of RANKL and OPG in a rat model of mechanical instability-induced peri-implant osteolysis. The rats were treated daily with a GSK-3β inhibitor, AR28 (20 mg/kg bw), for up to 5 days. Bone tissue and blood serum were assessed by qRT-PCR, immunohistochemistry and ELISA on days 3 and 5, and by micro-CT on day 5. After 3 days of treatment with AR28, mRNA levels of β-catenin, Runx2, Osterix, Col1α1 and ALP were increased leading to higher osteoblast numbers compared to vehicle-treated animals. BMP-2 and Wnt16 mRNA levels were downregulated by mechanical instability and this was rescued by GSK-3β inhibition. Osteoclast numbers were decreased significantly after 3 days of GSK-3β inhibition, which correlated with enhanced OPG mRNA expression. This was accompanied by decreased serum levels of TRAP5b on days 3 and 5. Treatment with AR28 upregulated osteoblast differentiation, while osteoclastogenesis was blunted, leading to increased bone mass by day 5. These data suggest that GSK-3β inactivation suppresses osteolysis through regulating both osteoblast and osteoclast differentiation in a rat model of instability-induced osteolysis.

**Corresponding Author:** Anna Fahlgren, **Tel**: +46 13 286710, **Fax**: +46 10 1034273, anna.fahlgren@liu.se.

**Disclosures:** The author(s) declared the following potential conflicts of interest with respect to the research, authorship, and/or publication of this article: AF, MA, RV, PR and MB declare that they have no competing interests. JE is an employee of AstraZeneca.

**Keywords**

Mechanical instability; Osteolysis; Bone implant; Wnt signaling; GSK-3β

## Introduction

The biological and mechanical processes involved in loosening of hip or knee prostheses are complex. Wear debris particles initiate inflammatory responses leading to differentiation of osteoclasts and peri-prosthetic bone loss. In addition to wear debris particles, fluid pressure fluctuations caused by implant instability in the peri-prosthetic tissue is a key factor in peri-prosthetic osteolysis and implant loosening. There is a strong inverse correlation between the amount of bone-implant contact and micromotion (Karrholm et al., 1994). At the peri-prosthetic interfaces, small gaps with very high fluid shear stress have been associated with increased bone resorption (Alidousti et al., 2011; Mann and Miller, 2014). In the peri-prosthetic tissue of loosened implants, higher ratios of osteoclast to osteoblast numbers are reported compared to stable prostheses (Kadoya et al., 1996). Imbalance between bone-degrading osteoclasts and bone-forming osteoblasts around implants, ultimately results in bone degradation and loosening of the implant.

The role of the Wnt signaling pathway in regulating bone mass has been studied extensively (Kubota et al., 2009). Many Wnt ligands and receptors have been reported to exert pro-anabolic effects on bone tissue primarily through the promotion of osteoblast differentiation (Baron and Kneissel, 2013). However, Wnt signaling also modulates osteoclast differentiation and bone resorption. Production of the osteoclastogenesis inhibitory factor osteoprotegerin (OPG) is a direct target of β-catenin transcriptional activation (Glass et al., 2005). In mice with the β-catenin gene postnatally deleted bone mass was low, which was explained by a suppressed osteoblast differentiation (Song et al., 2012). It was further shown that mice expressing a dominant active form of β-catenin in osteoblasts exhibited a high bone mass phenotype through suppressed osteoclast differentiation and bone resorption, rather than affecting bone formation (Glass et al., 2005).

Non-canonical Wnt5a stimulates osteoclastogenesis by enhancing RANK (receptor activator of nuclear factor kappa-B) expression on osteoclast precursors (Maeda et al., 2012). Recently, Wnt16 was shown to suppress osteoclastogenesis directly by blunting RANKL-induced upregulation of NFκB (nuclear factor kappa B) and NFATc1 (nuclear factor of activated T-cells, cytoplasmic 1) and also by upregulating OPG expression in osteoblasts (Moverare-Skrtic et al., 2014).

Bone cells respond to mechanical load by regulating Wnt/β-catenin signaling. Glycogen synthase kinase 3 beta (GSK-3β) is a central player in canonical Wnt signaling (Glass and Karsenty, 2007; Gordon and Nusse, 2006). GSK-3β together with axin, adenomatous polyposis coli (APC) and casein kinase 1 (CK1) form a complex that degrades β-catenin in the cytoplasm. Inactivation of GSK-3β leads to cytoplasmic accumulation and subsequently nuclear translocation of β-catenin (Baron and Kneissel, 2013), where it enhances a transcriptional-based increase in Runx2, a major transcription factor for osteoblast differentiation (Glass and Karsenty, 2007; Gordon and Nusse, 2006).

Mice deficient for GSK-3β showed increased β-catenin and Runx2 levels, which was associated with higher bone regeneration rate after injury compared to wild-type mice (Arioka et al., 2014). Moreover, following GSK-3β inhibition fractures healed quicker in rats with enhanced bone strength (Sisask et al., 2013).

However, reports on the effects of GSK-3β inactivation on osteoclast differentiation in rodent models are conflicting. The number of osteoclasts following GSK-3β inhibition has been reported to be either unaffected or decreased in OVX-induced osteoporosis (Kulkarni et al., 2006; Zahoor et al., 2014) and in wear debris-induced osteolysis (Geng et al., 2015). Osteoclast numbers in healthy bone was unaffected (Marsell et al., 2012) or slightly increased (Gambardella et al., 2011). These reports suggest that GSK-3β inhibition affects bone tissue differently depending on the pathologic state and the remodeling activity between osteoblasts and osteoclasts.

The effects of GSK-3β inactivation on mechanically instability-induced peri-prosthetic bone loss have not been studied. However, we previously demonstrated that administration of OPG fusion protein (OPG-Fc) completely blocked osteoclast differentiation and bone loss around the implant in a rat model of instability-induced osteolysis (Aspenberg et al., 2011). The cellular processes behind instability-induced osteolysis remain unclear. AR28 is a potent inhibitor of GSK-3β (Ki= 5 nM) with over 70-fold selectivity compared to other enzymes/targets and in cellular assays it causes β-catenin accumulation and osteoblast differentiation (Gambardella et al., 2011). *In vivo*, AR28 stimulates β-catenin nuclear translocation, osteoblast differentiation and bone formation in rodents (Gambardella et al., 2011; Gilmour et al., 2013). In this study, we used an established animal model of instability-induced prosthetic loosening (Fahlgren et al., 2010; Nilsson et al., 2012; Skripitz and Aspenberg, 2000) to test the hypothesis that short-term inhibition of GSK-3β using AR28 (also known as AZD2858) will reduce bone loss through a mechanism of altered regulation of both osteoclasts and osteoblasts.

## Materials and Methods

### Animals and experimental design

One hundred seven male Sprague-Dawley rats (360–480 g) were used in a previously validated animal model (Fahlgren et al., 2010; Skripitz and Aspenberg, 2000) of instability-induced prosthesis loosening (a schematic visualization of the animal model is available in the Supplementary materials: Fig. S1). The animals were randomly distributed into two major treatment groups. The first group received the GSK-3β inhibitor (AR28 synthesized at AstraZeneca R&D, Loughborough UK) (20 mg/kg bw/day, oral gavage), while the second group received vehicle (5ml/kg, deionized water adjusted to pH 3.5). AR28, at a dose of 20 mg/kg/day, was selected based on the pharmacokinetic profile which demonstrates plasma levels sufficient to inhibit the GSK-3β enzyme *in vivo* and alters bone turnover within several days of oral dosing in rats (Gilmour et al., 2013). All groups had a tibial implant surgically inserted. The animals were sacrificed at day 0 (with a stable tibial implant), or after exposure to loading episodes simulating mechanical instability and micromotion of implants twice a day for 3 or 5 days. In addition, to study the effects of AR28 in healthy

bone without surgery, a group of intact animals were treated for 5 days with AR28 (n=8) or vehicle (n=8) (Table 1).

Tibial bone tissue from underneath the pressure piston and intact bone from femur were harvested and processed for immunohistochemical evaluation and micro-CT (μCT) analysis (n=8/group) or for RNA isolation (n=7/group). Blood samples were collected upon sacrifice for analysis of P1NP (Procollagen type 1 N-terminal propeptide) and TRAP5b (tartrate-resistant acid phosphatase) levels in serum. All experiments were approved by the IACUC committee for animal experiments at Hospital for Special Surgery, New York, NY, USA.

## Animal model

Briefly, a titanium plate was fastened to the proximal tibia and a plug protruded into a milled depression in the bone cortex. After osseointegration for 5 weeks, the control plug in the plate was replaced by a piston, which could be moved perpendicularly to the bone surface. A 5-day latency period was allowed prior to initiation of loading, during which a fibrous tissue layer formed in the space between the piston and the bone surface. An 8 N transcutaneous force (0.1 MPa), at a frequency of 0.17 Hz, was applied for 2 minutes twice daily, for 3 and 5 days. The piston simulated implant micromotion during mechanical instability creating a pressurized fluid flow onto the underlying bone without touching the bone surface (Fahlgren et al., 2010; Skripitz and Aspenberg, 2000). Animals which were used as non-loaded controls had a stable implant and were sacrificed without undergoing loading (Fig. S1).

## Measurement of bone density by μCT

The harvested bone specimens were scanned using a Scanco μCT 35 system (Scanco Medical, Bassersdorf, Switzerland) with a resolution of 15 μm. μCT analysis was performed on tibial bone from underneath the implant, which had undergone loading, to determine the changes in trabecular and cortical bone induced by GSK-3β inactivation, and on femurs to determine possible systemic changes in healthy bone following inhibition of GSK-3β. Bone volume fraction (BV/TV) was measured in the zone underneath the tibial implant (Fig. 1A) in a volume defined by a 4-mm diameter and a 0.8 mm deep cylinder, whose geometric center was placed at the same position as that of the piston.

For the femurs, the cortical region of interest was defined as the 2.0-mm mid-diaphyseal region, directly below the third trochanter, which includes both the mid-diaphysis and more proximal cortical bone regions. Cortical bone measurements consisted of cross-sectional area (Tt.Ar), cortical bone area (Ct.Ar), cortical bone area fraction (Ct.Ar/Tt.Ar) and cortical thickness (Ct.Th). Trabecular measurements included bone volume fraction (BV/TV), trabecular number (Tb.N), trabecular thickness (Tb.Th) and trabecular separation (Tb.Sp).

## Immunohistochemistry

The bone specimens were fixed in a 4% paraformaldehyde solution for 48 hours. After decalcification in 10% formic acid, the specimens were embedded in paraffin. Transverse sections of 7 μm were deparaffinized, rehydrated and blocked for endogenous peroxidase with 3% $H_2O_2$ for 5 minutes, followed by 20 minutes of blocking with serum-free protein block (Dako Cytomation, Glostrup, Denmark), and 80 minutes incubation with biotinylated

rabbit anti-rat TRAP IgG (1:600) (Hollberg et al., 2005) or rabbit anti-mouse procollagen I monoclonal antibody (SP1.D8) (1:50) (DSHB, Cat# SP1.D8, RRID:AB_528438) and PCNA (1:100) (Santa Cruz Biotechnology, Cat# sc-56, RRID:AB_628110) and HRP-labeled secondary anti-mouse and anti-rabbit antibodies (Dako) for 30 minutes. Vectastain Elite ABC kit (Vector laboratories, Burlingame, CA, USA) was applied for 30 minutes prior to incubation with 3,3′diaminobenzidine (DAB) (Sigma, St Louis, MO, USA) for 5 minutes. All antibodies were diluted in real™ antibody diluent (Dako) and incubations were performed at room temperature.

### Histomorphometry and immunohistochemistry analysis

To visualize effects of GSK-3β inhibition on bone cells, the number of TRAP-positive osteoclasts and procollagen 1-positive osteoblasts were assessed by light microscopy. In the tibial tissue underneath the implant, histology analysis was performed on the area underneath the implant (Fig. 1B). In the distal femur, three zones (500 μm × 500 μm) were analyzed up to 300 μm underneath the epiphysis plate (Fig. 1C). Osteoclasts were counted in two representative sections at two levels of the bone separated by a 450 μm distance. Osteoclasts were defined as TRAP-positive multinucleated cells within a distance of 0.05 mm from the bone surface and data were expressed as the number of osteoclasts per bone surface. Mature osteoblasts were defined as procollagen 1-positive cells and used for histomorphometry. Proliferating osteoblasts were identified as proliferating cell nuclear antigen (PCNA)-positive cells, and were used for descriptive histology. Osteoblast perimeter was determined by measuring the perimeter of procollagen 1-positive cells per bone surface. The histomorphometric parameters, osteoclast numbers (N.Ocl), osteoblast perimeter (Ob.Pm) and bone surface area (BS) in tibia and femur were measured using OsteoMeasure™ Software version 3.3.0.2 (Osteometrics, Atlanta, GA, USA).

### Measurement of serum P1NP and TRAP5b by ELISA

Blood samples were collected through cardiac puncture from animals at the time of sacrifice for measurements of bone turnover markers in serum. P1NP (#AC-33F1), and TRAP5b (#SB-TR102) assays were used to quantitate osteoblast and osteoclast activity, respectively, using commercially available ELISA kits according to manufacturers' instructions (Immunodiagnostic Systems, Gaithersburg, MD, USA).

### Gene expression analysis

For RNA isolation, a custom-made trephine with diameter a of 4.5 mm was used to harvest bone tissue from the loaded areas in tibia. The specimens were rinsed with cold saline, and the bone marrow was carefully removed from the bone specimens. No periosteum was present since it was trimmed away during surgery. Samples were immediately snap-frozen in liquid Nitrogen for extraction of total RNA using the TRIspin method described previously (Nilsson et al., 2012). Cortical bone samples were harvested from the femur diaphysis for RNA extraction to investigate systemic effects of AR28 treatment. Primers for beta-catenin (Ctnnb1) (Rn00584431_g1), Runx2 (Rn01512298_m1), Osterix (Sp7) (Rn02769744_s1), ALP (Rn01516028_m1), Col1α1 (Rn01463848_m1), BMP-2 (Rn00567818_m1), Wnt16 (Rn01500994_m1), Wnt5a (Rn01402000_m1) RANKL (Tnfsf11) (Rn00589289_m1), OPG (Tnfrsf11b) (Rn00563499_m1) and 18S rRNA (Hs99999901_s1) were purchased from

Applied Biosystems. Reactions were performed in duplicate with TaqMan Fast Universal PCR Master Mix (Applied Biosystem, UK) using the standard curve methodology. All expression levels were normalized to 18S rRNA.

### Statistics

Statistical analyses were performed by Kruskall-Wallis ANOVA, followed by intergroup comparisons using the Mann-Whitney *U* test using SPSS Statistics 22.0. The intergroup comparisons were performed to compare 1) AR28 treatment versus vehicle at each time point and 2) AR28 versus control. Differences with $p<0.05$ were considered statistically significant.

## Results

### Inactivation of GSK-3β increases osteoblast proliferation and bone mass in rat tibia subjected to mechanical instability

To determine whether GSK-3β inactivation affects osteoblast differentiation and bone mass in bone subjected to instability, we treated animals with AR28 for 3 and 5 days and examined the bone underneath the implant.

Mechanical instability itself did not affect BV/TV at day 5 (Fig. 2A) compared to controls. At the cellular level, mechanical instability induced an increased Ob.Pm/BS at day 3 compared to controls, but the difference was absent at day 5 (Fig. 2B). Mechanical instability in the presence of the GSK-3β inhibitor AR28, led to an enhanced BV/TV compared to vehicle-treated animals and to controls (Fig. 2A). At the cellular level, 5 days of GSK-3β inhibition resulted in an increased Ob.Pm/BS (32.0 vs 13.6) compared to vehicle (Fig. 2B). The majority of PCNA-positive proliferative osteoblasts after 5 days of treatment were located within the marrow cavity, while procollagen 1-positive differentiated osteoblasts were seen at the surface of the newly formed bone (Fig. 2C).

No effect was found in intact femurs following 5 days of GSK-3β inhibition in any cortical (Tt.Ar, Ct.Ar, Ct.Ar/Tt.Ar, Ct.Th,) or trabecular (BV/TV, Tb.N, Tb.Th, Tb.Sp) bone parameters visualized by μCT or Ob.Pm/BS (%), compared to vehicle-treated animals (Fig. 2D, E). Finally, serum levels of P1NP were similar in AR28- or vehicle-treated animals at day 3 and 5 (Fig. 2F).

### GSK-3β inhibition increases mRNA expression of β-catenin and osteogenic markers

There were no detectable changes in mRNA levels of osteogenic markers in bone tissue subjected to instability compared to controls at day 3. However, at day 5 there was an increase in the mRNA expression of β-catenin and Col1α1 (Collagen, type I, alpha 1), while Runx2, Osterix and ALP were unaffected compared to controls.

Following GSK-3β inhibition in the presence of instability, all osteogenic markers, namely Runx2, Osterix, ALP and Col1α1 were significantly enhanced after 3 days compared to animals receiving vehicle (Fig. 3A–E). The early stimulatory effects of GSK-3β inhibition on mRNA levels of β-catenin and the osteogenic genes were not maintained in tibia at day 5 (Fig. 3A–E).

The mRNA expression of β-catenin, Runx2, Osterix, ALP and Col1α1 were all significantly upregulated in intact femurs following 5 days of GSK-3β inhibition compared to vehicle-treated animals (Fig. 3F–J).

### GSK-3β inhibition rescues instability-induced downregulation of BMP-2 and Wnt16 mRNA

Loading directly interferes with changes in the Wnt/β-catenin signaling pathway (Santos et al., 2009; Tella and Gallagher, 2014; van Amerongen et al., 2012). BMP-2 and Wnt/β-catenin signaling interact to enhance the expression of OPG. The active form of GSK-3β is a key negative regulator of Smad1/BMP-2 signaling and inhibits osteoblast differentiation (Biver et al., 2014; Sato et al., 2009).

The mRNA expression of BMP-2 and Wnt16 was downregulated in the bone subjected to instability in vehicle-treated animals compared to controls (Fig. 4A,B). The instability-induced suppression of BMP-2 and Wnt16 seen at day 3 disappeared at day 5, resulting in mRNA levels similar to those of controls (Fig. 4A,B). Following GSK-3β inhibition for 3 days, the decrease in mRNA levels of BMP-2 and Wnt16 by mechanical instability was rescued and changed to an increased expression compared to controls. At day 5 there were no changes in mRNA levels of BMP-2 and Wnt16 following GSK-3β inhibition.

Wnt5a mRNA expression was not affected by instability at day 3 but was upregulated by day 5 compared to controls. Inactivation of GSK-3β by AR28 did not change Wnt5a levels in comparison to vehicle-treated animals. However, AR28 administration upregulated Wnt5a mRNA at both days 3 and 5 compared to controls (Fig. 4C). Expression of BMP-2 mRNA was significantly increased in the intact femur following GSK-3β inhibition compared to the vehicle-treated animals, while those of Wnt16 and Wnt5a were unaffected (Fig. 4D–F).

### GSK-3β inhibition suppresses mechanical instability-induced osteoclast differentiation

There was a substantial increase in the number of osteoclasts underneath the tibial implant after 3 days of induction of mechanical instability, compared to non-loaded controls (Fig. 5A). At day 5, this effect was no longer present. Treatment with the GSK-3β inhibitor decreased the number of osteoclasts in the tibia subjected to instability at both days 3 and 5 compared to vehicle-treated animals (Fig. 5A).

When TRAP-positive osteoclasts were quantified in the intact femur at day 5, there was no significant suppression visible after administration of the GSK-3β inhibitor (Fig. 5B). GSK-3β inhibition with AR28 led to a significant reduction in TRAP5b serum levels by 23% after 3 days, and by 54% after 5 days compared to vehicle-treated animals subjected to instability (Fig. 5C). Intact animals without surgery had a 43% decrease in the TRAP5b serum levels with AR28 treatment compared to vehicle-treated animals.

### Suppression of instability-induced osteoclastogenesis correlates to a decrease in the RANKL/OPG ratio

Mechanical instability induced an increase in tibial mRNA levels of both RANKL (1.3-fold) and OPG (1.7-fold) at day 3, but there was no change in the RANKL/OPG ratio. In contrast, the GSK-3β inhibitor induced a 2.4-fold rise in OPG expression with no change in RANKL

levels leading to a decreased RANKL/OPG ratio by 50% compared to vehicle-treated animals (Fig. 6A–C). At day 5 this effect was no longer found.

In intact femurs, GSK-3β inhibition induced an upregulation in both RANKL (2.2-fold) and OPG (1.6-fold) after 5 days of AR28 treatment, resulting in a tendency towards an increased RANKL/OPG ratio (1.3-fold) (Fig. 6D–F).

## Discussion

Stimulating the Wnt/β-catenin signaling pathway has been proposed as a promising approach to develop bone anabolic therapeutics (Baron and Kneissel, 2013; Tella and Gallagher, 2014). However, little is known about the role of Wnt/β-catenin signaling in mechanical instability-induced peri-prosthetic bone loss. It was recently shown that GSK-3β has direct effects on both osteoblasts and osteoclasts and thus on bone mass (Gambardella et al., 2011; Geng et al., 2015; Gilmour et al., 2013; Marsell et al., 2012; Sisask et al., 2013; Zahoor et al., 2014). In this study, we found that inhibition of GSK-3β for 5 days accelerated bone repair by regulating both osteoblast and osteoclast differentiation in a model of instability-induced peri-prosthetic bone loss (Fig. 7).

We detected enhanced β-catenin gene expression after GSK-3β inhibition with AR28, which was associated with an early increase in expression of Runx2 and Osterix, as well as markers for osteoblast activity such as ALP and procollagen 1 at day 3. These changes in osteogenic markers were followed by increased numbers of osteoblasts and bone mass in the tibial bone subjected to instability at day 5. The increase in osteoblast differentiation following AR28 treatment is in agreement with previous *in vitro* and *in vivo* studies using the same GSK-3β inhibitor (Abu-Amer et al., 2007; Gambardella et al., 2011; Gilmour et al., 2013; Marsell et al., 2012; Sisask et al., 2013), but also similar to data from knockout mice with deletion of GSK-3β. In healthy rodents, GSK-3β inhibition promoted β-catenin nuclear translocation (Gambardella et al., 2011), increased mRNA expression of osteoblastogenesis markers (Kulkarni et al., 2006) and enhanced bone mass and mineral apposition rate (Gambardella et al., 2011; Gilmour et al., 2013; Marsell et al., 2012). Our data also show that inactivation of GSK-3β mediates a strong bone-anabolic effect in peri-prosthetic tissue subjected to mechanical instability.

Modulating Wnt/β-catenin signaling, through GSK-3β inactivation can also affect osteoclast differentiation. In this study, osteoclast numbers per bone surface area were decreased following GSK-3β inhibition for 3 and 5 days in bone exposed to instability, but not in intact bone. The anti-catabolic effects were confirmed by decreased serum levels of TRAP5b on days 3 and 5. A decline in bone resorption systemic markers such as CTX-1 (Marsell et al., 2012) and TRAP5b (Gilmour et al., 2013) after GSK-3β inhibition have been reported previously. GSK-3β inhibition has further been shown to suppress wear debris-induced osteolysis (Geng et al., 2015) and OVX-induced osteoporosis (Zahoor et al., 2014), while it has been reported ineffective on osteoclast differentiation in OVX-induced osteoporosis (Kulkarni et al., 2006) and in healthy rodents (Marsell et al., 2012). The contradictory reports regarding osteoclast differentiation after inhibition of GSK-3β could be related to

several factors such as species, treatment duration, and relative potency of different compounds but also to the pathologic state of bone tissue.

Several mechanisms related to β-catenin signaling are suggested to modulate RANK-RANKL-OPG signaling in osteoclasts, which are mainly controlled by other cell types such as osteoblasts and osteocytes. In this study, GSK-3β inhibition suppressed osteoclastogenesis, which was associated with a decrease in RANKL/OPG mRNA ratio at day 3, resulting from increased OPG. This implicates the direct involvement of osteoblast in mechanically instability-induced osteolysis. This is in line with previous results showing a significant protection against instability-induced bone resorption in animals by a recombinant OPG-Fc, which acts as a RANKL neutralizing monoclonal antibody (Aspenberg et al., 2011). OPG, which disrupts the RANK-RANKL axis, is secreted by osteoblasts, and is one of the target genes in β-catenin-dependent transcription. (Biver et al., 2014; Sato et al., 2009; Yan et al., 2009).

We found both Wnt16 and BMP-2 downregulated following induction of mechanical instability, and this was rescued by GSK-3β inactivation (Fig. 4). Deletion of the Wnt16 gene in mice resulted in more osteoclasts and low cortical mass (Moverare-Skrtic et al., 2014). The mechanism for a mechanoresponsive role of Wnt16 is still unclear. Mechanical strain induced significantly higher cross-sectional cortical area (Wergedal et al., 2015), while mechanical unloading did not induce any changes (Todd et al., 2015). It has been suggested that other targets in the Wnt/β-catenin signaling might be associated with Wnt16, which exert compensatory effects in presence of loading (Glass and Karsenty, 2007; Gordon and Nusse, 2006).

Wnt and BMP signaling pathways are two major targets under investigation to develop preventive measures for aseptic loosening of implants (Lee et al., 2013; Liu et al., 2012; Shah et al., 2013). The crosstalk between Wnt and BMP signaling is complex and both synergy and antagonism between them have been reported. However, they both appear to positively cooperate in contributing to osteoblast differentiation (Baron and Kneissel, 2013). BMP-2 is one of the most potent inducers of mesenchymal progenitor cell differentiation into osteoblasts and is modulated by mechanical loading (McBride et al., 2014). There is evidence that BMP-2 regulates osteoblast differentiation and OPG production through a GSK-3β-dependent mechanism (Fukuda et al., 2010; Sato et al., 2009). In vitro studies have shown that BMP-2-induced expression of osteoblast markers needs activity of Wnt/β-catenin signaling (Rawadi et al., 2003; Silverio et al., 2012). Suppressed osteoblast differentiation has been rescued by administration of the GSK-3β inhibitor (2′Z,3′E)-6-Bromoindirubin-3′-oxime (BIO), through a β-catenin-BMP-2/4-dependent upregulation of osteogenic genes and OPG (Yan et al., 2009). Previous studies and our data suggest a close interaction between β-catenin/GSK-3β signaling and BMP-2, in an OPG-dependent manner.

Wnt5a, which is expressed by osteoblasts, stimulates RANKL-induced osteoclast differentiation. The upregulation of Wnt5a after 3 days of AR28 treatment in presence of mechanical loading could be related to increased osteoblast differentiation. Although Wnt5a and Wnt16 act through different signaling pathways, Wnt5a is reported to repress the inhibitory effects of Wnt16 on osteoclast differentiation (Kobayashi et al., 2015). Wnt5a

itself has been reported to promote osteoblast differentiation instead of adipogenesis (Takada et al., 2014). This might act to compensate for bone resorption around the implant. However, here the specific role of Wnt5a appears to be minor, since the net effect is decrease in osteoclast differentiation.

In this study, in an animal model of instability-induced prosthetic loosening, GSK-3β inhibition induced a transient increase in bone formation and blunted bone degradation. The early onset of bone remodeling underneath an unstable implant could be related to the high metabolic activity in the bone tissue subjected to loading in the tibia compared to the intact femur. It could also be explained by the difference between osteolytic and intact bone. During bone remodeling of intact bone, osteoprogenitors activate the process of coupling between resorption and formation. However, uncoupling between osteoblasts and osteoclasts has been shown in osseointegration of bone implants and in fracture healing, which also have a high active metabolic rate (Aspenberg et al., 2008).

In conclusion, our data show that GSK-3β inactivation suppresses osteolysis induced by mechanical instability of implants. Our findings suggest that GSK-3β signaling regulates both osteoblast and osteoclast differentiation, and its inactivation leads to enhanced bone mass, in a rat model of mechanically induced osteolysis. Although modulation of Wnt/β-catenin signaling has been suggested for treatment of several bone metabolic diseases, pharmaceutical agents that mitigate ongoing aseptic loosening are not yet available. Blocking GSK-3β, a pivotal molecule in the Wnt/β-catenin signaling cascade, might be a promising treatment strategy to delay or prevent aseptic prosthetic loosening, since it acts through both pro-anabolic and anti-catabolic mechanisms. Inhibition of GSK-3β, for short treatment periods, might be used advantageously by local administration (Arioka et al., 2014) for instance through use of implants coated with a GSK-3β inhibitor, to avoid potential systemic side effects.

## Supplementary Material

Refer to Web version on PubMed Central for supplementary material.

## Acknowledgments

This study was supported by funding agencies in Sweden including the Swedish Research Council (K2014-7X-22506-01-3 to AF), Swedish Governmental Agency for Innovation Systems (2012-04409 to AF) and the National Institutes of Health (AR056802 to MB).

**Grants**: Swedish Research Council (K2014-7X-22506-01-3); Swedish Governmental Agency for Innovation Systems (VINNOVA: 2012-04409) and National Institutes of Health (NIH: AR056802).

## References

Abu-Amer Y, Darwech I, Clohisy JC. Aseptic loosening of total joint replacements: mechanisms underlying osteolysis and potential therapies. Arthritis Res Ther. 2007; 9

Alidousti H, Taylor M, Bressloff NW. Do Capsular Pressure and Implant Motion Interact to Cause High Pressure in the Periprosthetic Bone in Total Hip Replacement? J Biomech Eng-T Asme. 2011; 133(12)

Arioka M, Takahashi-Yanaga F, Sasaki M, Yoshihara T, Morimoto S, Hirata M, Mori Y, Sasaguri T. Acceleration of bone regeneration by local application of lithium: Wnt signal-mediated

osteoblastogenesis and Wnt signal-independent suppression of osteoclastogenesis (vol 90, pg 397, 2014). Biochem Pharmacol. 2014; 91(4):552–553.

Aspenberg P, Agholme F, Magnusson P, Fahlgren A. Targeting RANKL for reduction of bone loss around unstable implants: OPG-Fc compared to alendronate in a model for mechanically induced loosening. Bone. 2011; 48(2):225–230. [PubMed: 20858557]

Aspenberg P, Wermelin K, Tengwall P, Fahlgren A. Additive effects of PTH and bisphosphonates on the bone healing response to metaphyseal implants in rats. Acta orthopaedica. 2008; 79(1):111–115. [PubMed: 18283582]

Baron R, Kneissel M. WNT signaling in bone homeostasis and disease: from human mutations to treatments. Nat Med. 2013; 19(2):179–192. [PubMed: 23389618]

Biver E, Thouverey C, Magne D, Caverzasio J. Crosstalk between tyrosine kinase receptors, GSK3 and BMP2 signaling during osteoblastic differentiation of human mesenchymal stem cells. Mol Cell Endocrinol. 2014; 382(1):120–130. [PubMed: 24060635]

Fahlgren A, Bostrom MP, Yang X, Johansson L, Edlund U, Agholme F, Aspenberg P. Fluid pressure and flow as a cause of bone resorption. Acta orthopaedica. 2010; 81(4):508–516. [PubMed: 20718695]

Fukuda T, Kokabu S, Ohte S, Sasanuma H, Kanomata K, Yoneyama K, Kato H, Akita M, Oda H, Katagiri T. Canonical Wnts and BMPs cooperatively induce osteoblastic differentiation through a GSK3 beta-dependent and beta-catenin-independent mechanism. Differentiation. 2010; 80(1):46–52. [PubMed: 20546990]

Gambardella A, Nagaraju CK, O'Shea PJ, Mohanty ST, Kottam L, Pilling J, Sullivan M, Djerbi M, Koopmann W, Croucher PI, Bellantuono I. Glycogen Synthase Kinase-3 alpha/beta Inhibition Promotes In Vivo Amplification of Endogenous Mesenchymal Progenitors With Osteogenic and Adipogenic Potential and Their Differentiation to the Osteogenic Lineage. Journal of Bone and Mineral Research. 2011; 26(4):811–821. [PubMed: 20939016]

Geng DC, Wu J, Shao HG, Zhu SJ, Wang YJ, Zhang W, Ping ZC, Hu XY, Zhu XS, Xu YZ, Yang HL. Pharmaceutical inhibition of glycogen synthetase kinase 3 beta suppresses wear debris-induced osteolysis. Biomaterials. 2015; 69:12–21. [PubMed: 26275858]

Gilmour PS, O'Shea PJ, Fagura M, Pilling JE, Sanganee H, Wada H, Courtney PF, Kavanagh S, Hall PA, Escott KJ. Human stem cell osteoblastogenesis mediated by novel glycogen synthase kinase 3 inhibitors induces bone formation and a unique bone turnover biomarker profile in rats. Toxicol Appl Pharm. 2013; 272(2):399–407.

Glass DA, Bialek P, Ahn JD, Starbuck M, Patel MS, Clevers H, Taketo MM, Long FX, McMahon AP, Lang RA, Karsenty G. Canonical Wnt signaling in differentiated osteoblasts controls osteoclast differentiation. Dev Cell. 2005; 8(5):751–764. [PubMed: 15866165]

Glass DA, Karsenty G. Minireview: In vivo analysis of Wnt signaling in bone. Endocrinology. 2007; 148(6):2630–2634. [PubMed: 17395705]

Gordon MD, Nusse R. Wnt signaling: Multiple pathways, multiple receptors, and multiple transcription factors. Journal of Biological Chemistry. 2006; 281(32):22429–22433. [PubMed: 16793760]

Hollberg K, Nordahl J, Hultenby K, Mengarelli-Widholm S, Andersson G, Reinholt FP. Polarization and secretion of cathepsin K precede tartrate-resistant acid phosphatase secretion to the ruffled border area during the activation of matrix-resorbing clasts. J Bone Miner Metab. 2005; 23(6): 441–449. [PubMed: 16261450]

Kadoya Y, Revell PA, al-Saffar N, Kobayashi A, Scott G, Freeman MA. Bone formation and bone resorption in failed total joint arthroplasties: histomorphometric analysis with histochemical and immunohistochemical technique. J Orthop Res. 1996; 14(3):473–482. [PubMed: 8676261]

Karrholm J, Borssen B, Lowenhielm G, Snorrason F. Does Early Micromotion of Femoral Stem Prostheses Matter - 4-7-Year Stereoradiographic Follow-up of 84 Cemented Prostheses. Journal of Bone and Joint Surgery-British Volume. 1994; 76b(6):912–917.

Kobayashi Y, Thirukonda GJ, Nakamura Y, Koide M, Yamashita T, Uehara S, Kato H, Udagawa N, Takahashi N. Wnt16 regulates osteoclast differentiation in conjunction with Wnt5a. Biochem Bioph Res Co. 2015; 463(4):1278–1283.

Kubota T, Michigami T, Ozono K. Wnt signaling in bone metabolism. J Bone Miner Metab. 2009; 27(3):265–271. [PubMed: 19333681]

Kulkarni NH, Onyia JE, Zeng QQ, Tian XY, Liu M, Halladay DL, Frolik CA, Engler T, Wei T, Kriauciunas A, Martin TJ, Sato M, Bryant HU, Ma YFL. Orally bioavailable GSK-3 alpha/beta dual inhibitor increases markers of cellular differentiation in vitro and bone mass in vivo. Journal of Bone and Mineral Research. 2006; 21(6):910–920. [PubMed: 16753022]

Lee HJ, Koo AN, Lee SW, Lee MH, Lee SC. Catechol-functionalized adhesive polymer nanoparticles for controlled local release of bone morphogenetic protein-2 from titanium surface. J Control Release. 2013; 170(2):198–208. [PubMed: 23727196]

Liu S, Virdi AS, Sena K, Sumner DR. Sclerostin Antibody Prevents Particle-Induced Implant Loosening by Stimulating Bone Formation and Inhibiting Bone Resorption in a Rat Model. Arthritis and rheumatism. 2012; 64(12):4012–4020. [PubMed: 23192793]

Maeda K, Kobayashi Y, Udagawa N, Uehara S, Ishihara A, Mizoguchi T, Kikuchi Y, Takada I, Kato S, Kani S, Nishita M, Marumo K, Martin TJ, Minami Y, Takahashi N. Wnt5a-Ror2 signaling between osteoblast-lineage cells and osteoclast precursors enhances osteoclastogenesis. Nat Med. 2012; 18(3):405–U166. [PubMed: 22344299]

Mann KA, Miller MA. Fluid-structure interactions in micro-interlocked regions of the cement-bone interface. Computer methods in biomechanics and biomedical engineering. 2014; 17(16):1809–1820. [PubMed: 23480611]

Marsell R, Sisask G, Nilsson Y, Sundgren-Andersson AK, Andersson U, Larsson S, Nilsson O, Ljunggren O, Jonsson KB. GSK-3 inhibition by an orally active small molecule increases bone mass in rats. Bone. 2012; 50(3):619–627. [PubMed: 22142634]

McBride SH, McKenzie JA, Bedrick BS, Kuhlmann P, Pasteris JD, Rosen V, Silva MJ. Long Bone Structure and Strength Depend on BMP2 from Osteoblasts and Osteocytes, but Not Vascular Endothelial Cells. Plos One. 2014; 9(5)

Moverare-Skrtic S, Henning P, Liu XW, Nagano K, Saito H, Borjesson AE, Sjogren K, Windahl SH, Farman H, Kindlund B, Engdahl C, Koskela A, Zhang FP, Eriksson EE, Zaman F, Hammarstedt A, Isaksson H, Bally M, Kassem A, Lindholm C, Sandberg O, Aspenberg P, Savendahl L, Feng JQ, Tuckermann J, Tuukkanen J, Poutanen M, Baron R, Lerner UH, Gori F, Ohlsson C. Osteoblast-derived WNT16 represses osteoclastogenesis and prevents cortical bone fragility fractures. Nat Med. 2014; 20(11):1279–1288. [PubMed: 25306233]

Nilsson A, Norgard M, Andersson G, Fahlgren A. Fluid pressure induces osteoclast differentiation comparably to titanium particles but through a molecular pathway only partly involving TNFa. J Cell Biochem. 2012; 113(4):1224–1234. [PubMed: 22095724]

Rawadi G, Vayssiere B, Dunn F, Baron R, Roman-Roman S. BMP-2 controls alkaline phosphatase expression and osteoblast mineralization by a Wnt autocrine loop. Journal of Bone and Mineral Research. 2003; 18(10):1842–1853. [PubMed: 14584895]

Santos A, Bakker AD, Zandieh-Doulabi B, Semeins CM, Klein-Nulend L. Pulsating Fluid Flow Modulates Gene Expression of Proteins Involved in Wnt Signaling Pathways in Osteocytes. J Orthopaed Res. 2009; 27(10):1280–1287.

Sato MM, Nakashima A, Nashimoto M, Yawaka Y, Tamura M. Bone morphogenetic protein-2 enhances Wnt/beta-catenin signaling-induced osteoprotegerin expression. Genes Cells. 2009; 14(2):141–153. [PubMed: 19170762]

Shah NJ, Hyder MN, Moskowitz JS, Quadir MA, Morton SW, Seeherman HJ, Padera RF, Spector M, Hammond PT. Surface-Mediated Bone Tissue Morphogenesis from Tunable Nanolayered Implant Coatings. Sci Transl Med. 2013; 5(191)

Silverio KG, Davidson KC, James RG, Adams AM, Foster BL, Nociti FH, Somerman MJ, Moon RT. Wnt/beta-catenin pathway regulates bone morphogenetic protein (BMP2)-mediated differentiation of dental follicle cells. J Periodontal Res. 2012; 47(3):309–319. [PubMed: 22150562]

Sisask G, Marsell R, Sundgren-Andersson A, Larsson S, Nilsson O, Ljunggren O, Jonsson KB. Rats treated with AZD2858, a GSK3 inhibitor, heal fractures rapidly without endochondral bone formation. Bone. 2013; 54(1):126–132. [PubMed: 23337038]

Skripitz R, Aspenberg P. Pressure-induced periprosthetic osteolysis: a rat model. J Orthop Res. 2000; 18(3):481–484. [PubMed: 10937637]

Song LG, Liu ML, Ono N, Bringhurst FR, Kronenberg HM, Guo J. Loss of Wnt/beta-Catenin Signaling Causes Cell Fate Shift of Preosteoblasts From Osteoblasts to Adipocytes. Journal of Bone and Mineral Research. 2012; 27(11):2344–2358. [PubMed: 22729939]

Takada I, Mihara M, Suzawa M, Ohtake F, Kobayashi S, Igarashi M, Youn MY, Takeyama K, Nakamura T, Mezaki Y, Takezawa S, Yogiashi Y, Kitagawa H, Yamada G, Takada S, Minami Y, Shibuya H, Matsumoto K, Kato S. A histone lysine methyltransferase activated by non-canonical Wnt signalling suppresses PPAR-gamma transactivation (vol 9, pg 1273, 2007). Nat Cell Biol. 2014; 16(11):1126–1126.

Tella SH, Gallagher JC. Biological agents in management of osteoporosis. Eur J Clin Pharmacol. 2014; 70(11):1291–1301. [PubMed: 25204309]

Todd H, Galea GL, Meakin LB, Delisser PJ, Lanyon LE, Windahl SH, Price JS. Wnt16 Is Associated with Age-Related Bone Loss and Estrogen Withdrawal in Murine Bone. Plos One. 2015; 10(10)

van Amerongen R, Fuerer C, Mizutani M, Nusse R. Wnt5a can both activate and repress Wnt/beta-catenin signaling during mouse embryonic development. Dev Biol. 2012; 369(1):101–114. [PubMed: 22771246]

Wergedal JE, Kesavan C, Brommage R, Das S, Mohan S. Role of WNT16 in the Regulation of Periosteal Bone Formation in Female Mice. Endocrinology. 2015; 156(3):1023–1032. [PubMed: 25521583]

Yan Y, Tang DZ, Chen M, Huang J, Xie R, Jonason JH, Tan XH, Hou W, Reynolds D, Hsu W, Harris SE, Puzas JE, Awad H, O'Keefe RJ, Boyce BF, Chen D. Axin2 controls bone remodeling through the beta-catenin-BMP signaling pathway in adult mice. J Cell Sci. 2009; 122(19):3566–3578. [PubMed: 19737815]

Zahoor M, Cha PH, Min DS, Choi KY. Indirubin-3′-Oxime Reverses Bone Loss in Ovariectomized and Hindlimb-Unloaded Mice Via Activation of the Wnt/beta-Catenin Signaling. Journal of Bone and Mineral Research. 2014; 29(5):1196–1205. [PubMed: 24243753]

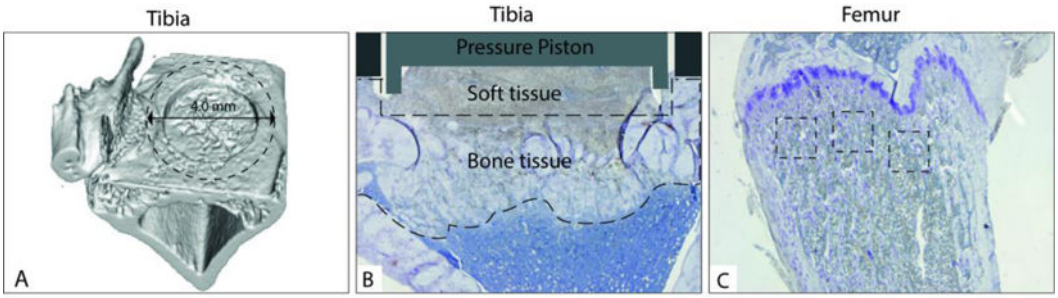


**Figure 1.**

Illustration of **A**) the micro-CT volume that was used to analyze the BV/TV underneath the implant, **B**) the area in the tibia underneath the pressure piston and **C**) that in the proximal femur underneath the growth plate, where the number of tartrate-resistant acid phosphatase (TRAP)-positive osteoclasts and procollagen 1-positive osteoblasts were assessed by light microscopy.

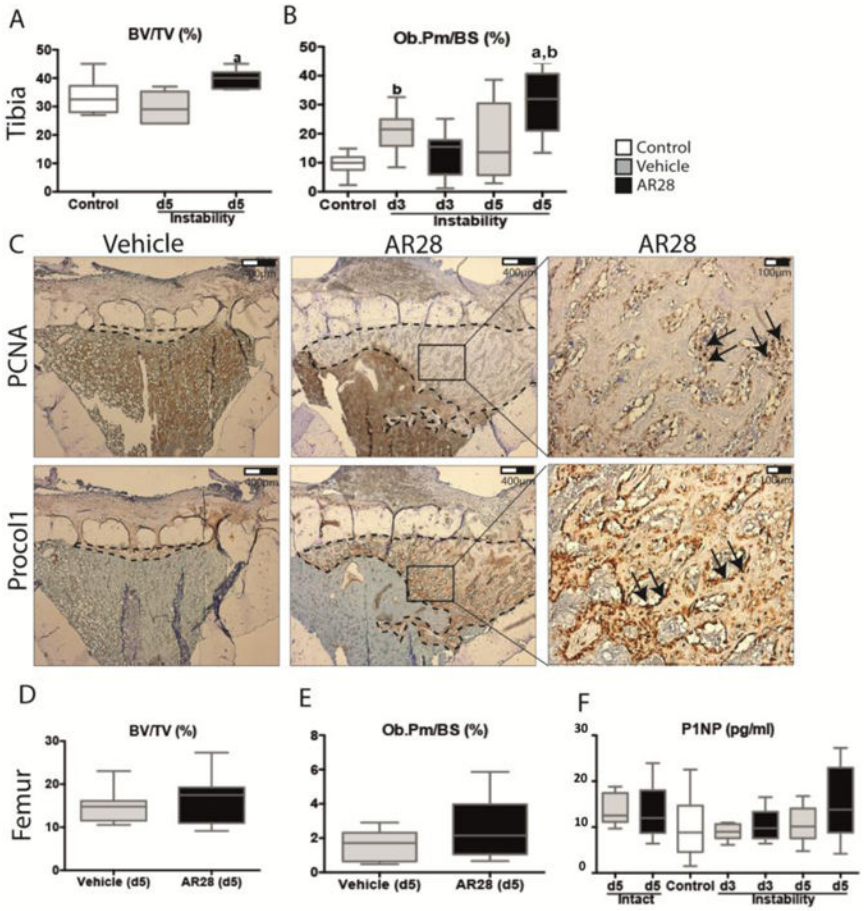


**Figure 2.**

GSK-3β inhibition increases osteoblast proliferation, differentiation and bone mass in the osteolytic bone tissue under the implant while the intact bone was unaffected. Micro-CT analysis and histomorphometry of tibia subjected to instability and femur after GSK-3β inhibition compared to vehicle and controls. (**A**) shows micro-CT analysis and (**B**) Ob.Pm/BS for tibial bones subjected to instability and (**C**) shows representative histological sections with PCNA and Procollagen 1-positive osteoblasts by GSK-3β inhibition compared to vehicle. (**D**) shows micro-CT and (**E**) Ob.Pm/BS in femur after 5 days of GSK-3β inhibition or vehicle. (**F**) shows serum levels of P1NP in controls and at 3 and 5 days after GSK-3β inhibition in intact animals and in presence of surgery. Boxplots indicate median as well as maximum and minimum in each group. **a**: significant compared to vehicle-treated animals, **b**: significant compared to controls. A p-value of <0.05 was considered significant.

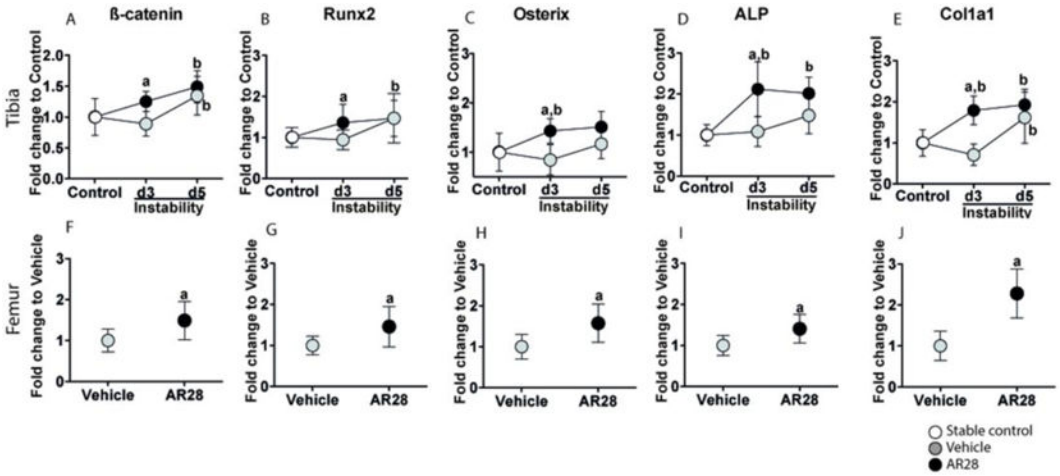


**Figure 3.**

GSK-3β inhibition increases mRNA expression of β-catenin and osteogenic markers in both the tibial bone underneath the implant and intact femur. Relative mRNA expression of β-catenin (**A**, **F**), Runx2 (**B**, **G**), Osterix (**C**, **H**), ALP (**D**, **I**) and Col1α1 (**E**, **J**) in tibial bone subjected to instability (upper panels) and intact femoral shaft (lower panels). Results are presented as the fold-change in tibial mRNA values compared to non-loaded controls (0 days) in bone harvested from animals subjected to instability or femoral mRNA in vehicle-treated animals. Graphs indicate mean±SD in each group. **a**: significant compared to vehicle-treated animals, **b**: significant changes compared to controls. A p-value of <0.05 was considered significant.

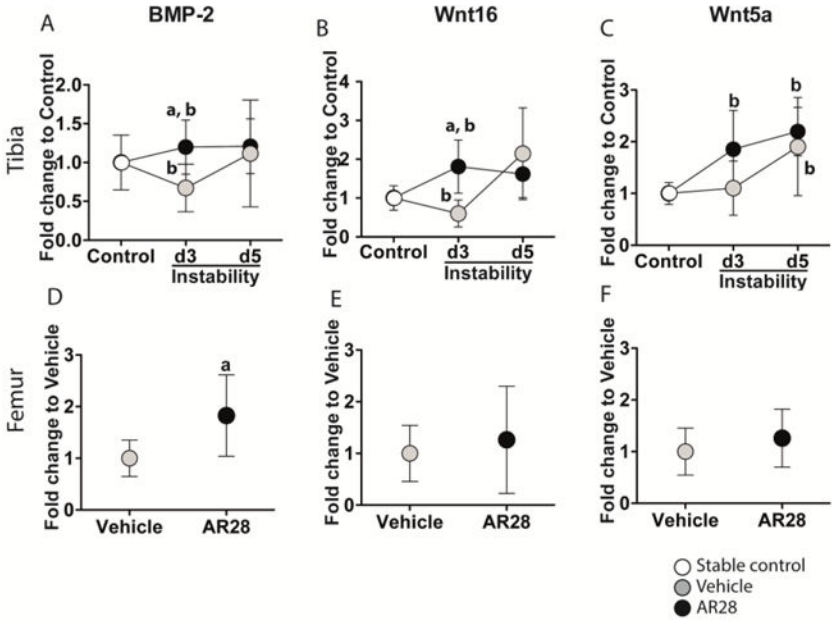


**Figure 4.**

GSK-3β inhibition rescues the instability-induced downregulation of BMP-2 and Wnt16 mRNA in bone tissue underneath the implant. Relative mRNA expression of BMP-2 (**A**, **D**), Wnt16 (**B**, **E**), and Wnt5a (**C**, **F**) in the tibial implant bone (upper panels) and the intact bone in femoral bone (lower panels). Results are expressed as the fold-change of mRNA expression in the tibia compared to that in controls (0 days) and to vehicle-treated animals in the femur. Graphs indicate mean±SD in each group. **a**: significant compared to vehicle-treated animals, **b**: significant changes compared to controls. A p-value of <0.05 was considered significant.

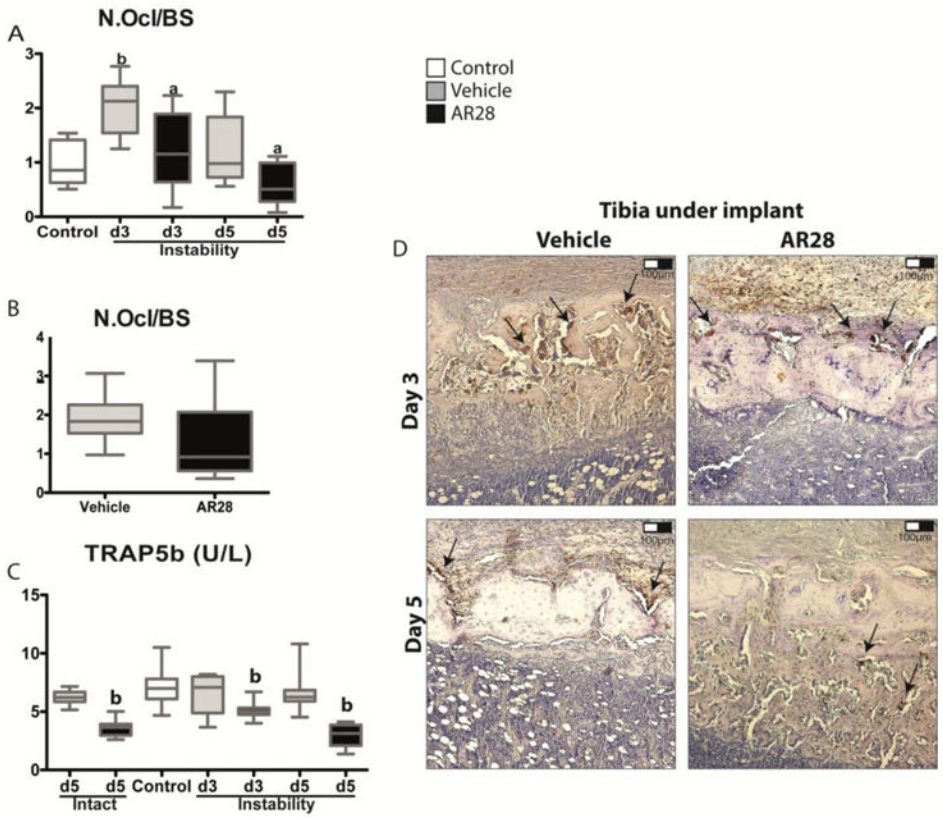


**Figure 5.**

GSK-3β inhibition decreases the number of osteoclasts in tibial bone underneath the implant but not in the intact femoral bone. Measurements of osteoclast number per bone surface in the tibial implant bone (**A**) and the intact femoral bone (**B**). Analysis of the serum levels of TRAP5b by ELISA at 0, 3 and 5 days (**C**). Representative TRAP immunohistochemistry of tibial bone under the implant at days 3 and 5 (**D**). Boxplots indicate median as well as maximum and minimum in each group. **a**: significant compared to vehicle-treated animals, **b**: significant changes compared to controls. A p-value of <0.05 was considered significant.

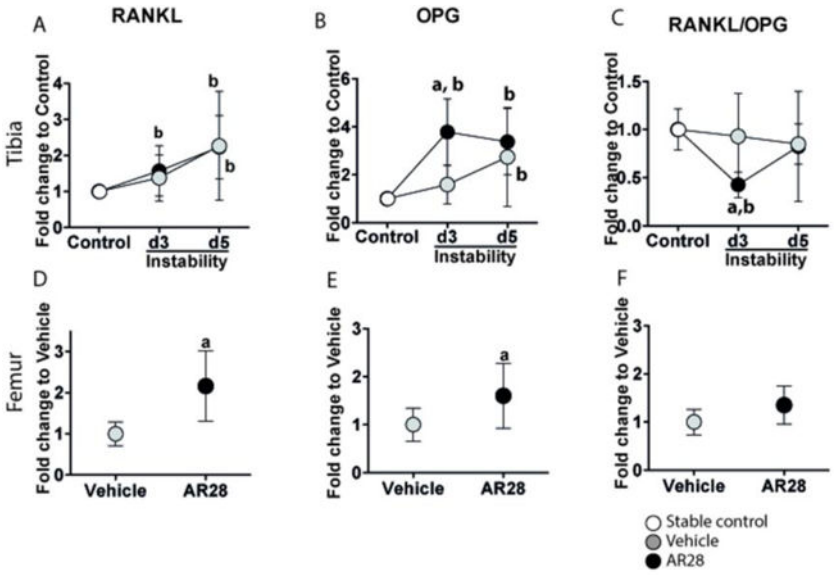


**Figure 6.**

GSK-3β inhibition suppresses osteoclast differentiation in an OPG-associated manner in the bone underneath the implant. Relative mRNA expression of RANKL (**A**, **D**), OPG (**B**, **E**) and RANKL/OPG ratio (**C**, **F**) in the tibial implant bone (upper panels) and intact femoral bone (lower panels). Results are presented as the fold-change in mRNA values compared to the non-loaded controls (0 days) in tibial bone and to vehicle-treated animals in femoral bone. Graphs indicate mean±SD in each group. **a**: significant compared to vehicle-treated animals, **b**: significant changes compared to controls. A p-value of <0.05 was considered significant.

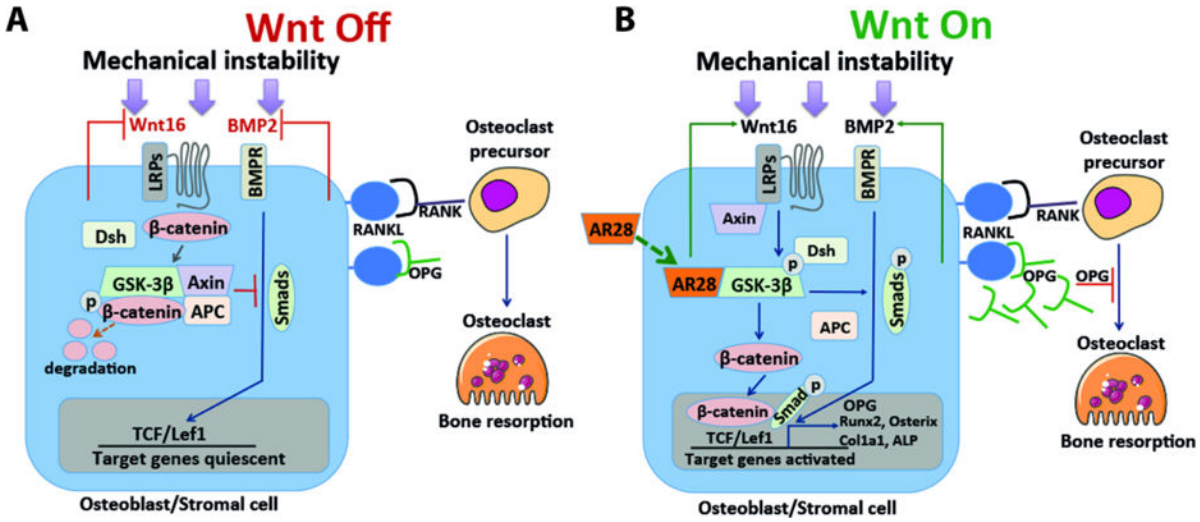


**Figure 7.**

Schematic model of proposed mechanism where GSK-3β signaling regulates both osteoblast and osteoclast differentiation in instability-induced osteoclast differentiation. **A**) Off-state of Wnt and BMP-2 signaling in absence of the GSK-3β inhibitor. **B**) On-state of Wnt and BMP-2 signaling in presence of the GSK-3β inhibitor. GSK-3β inhibition abrogates instability-induced osteoclast differentiation through Wnt16 and BMP-2 via an OPG-associated mechanism.

**Table 1**

Number of animals used for each analysis per group.

| | | No. of animals | No. of samples for each analysis | | | |
|---|---|---|---|---|---|---|
| | **Group** | **Total** | **qPCR** | **µCT** | **IHC*** | **ELISA**** |
| **Implant instability (Tibia)** | Control | 15 | 7 | 8 | 6† | 11 |
| | Vehicle (d3) | 15 | 7 | – | 8 | 11 |
| | AR28 (d3) | 15 | 6† | – | 8 | 12 |
| | Vehicle (d5) | 15 | 7 | 8 | 8 | 11 |
| | AR28 (d5) | 15 | 4† | 8 | 7† | 12 |
| **Intact animals (Femur)** | Vehicle (d5) | 16 | 8 | 8 | 7† | 11 |
| | AR28 (d5) | 16 | 8 | 8 | 8 | 12 |

**qPCR**: quantitative polymerase chain reaction; **µCT**: micro-computed tomography; **IHC**: Immunohistochemistry; **ELISA**: Enzyme-linked immunosorbent assay.

*: Samples used for µCT and IHC analyses were collected from the same animals.

**: Blood samples used for ELISA were collected randomly from animals in IHC and qPCR groups.

†: Samples excluded due to technical problems during sample processing.